Belg. J. Zool., 143(1) : 79-91 January 2013

Kinematic analysis of swimming ontogeny in seabass (*Dicentrarchus labrax*)

Damien Olivier[1,*], Quentin Mauguit[1], Nicolas Vandewalle[2] & Eric Parmentier[1]

[1] Laboratoire de Morphologie Fonctionnelle et Evolutive, Allée de la chimie, 3 Bât B6 Université de Liège, B-4000 Liège, Belgium.
[2] GRASP, Institut de Physique, Bât. B5a, Université de Liège, B-4000 Liège, Belgium.

* Corresponding author: dolivier@ulg.ac.be, tel : 0032(0)43665133, fax : 0032(0)43663715

ABSTRACT. Swimming has been investigated in multiple species, but few studies consider the establishment of swimming through ontogeny. This study describes the establishment of cyclical swimming in *Dicentrachus labrax*, a marine fish from cold, temperate waters. The data were compared with results from previous studies on two subtropical freshwater catfish species (*Clarias gariepinus* and *Corydoras aeneus*). The three species have different modes of locomotion each during their adult stage (anguilliform, subacarangiform and carangiform). The swimming of *Dicentrarchus labrax* was recorded with a high-speed video camera (500 fps) from 0 to 288 hours and from 960 to 2496 hours post-hatching. Three indices, i.e. coefficient of determination (r^2), coefficient of variation (CV), and Strouhal number (*St*), were used to investigate the establishment and efficiency of swimming. Important differences in the timing of swimming establishment were observed between the seabass and the two catfish species. The two catfish species display a sine-shaped swimming mode immediately or soon after hatching, and the efficiency of movement substantially improves during the first days of life. For seabass, however, establishment of swimming is slower during the same developmental period. These differences may be related to a faster developmental rate in the catfishes that allows them to swim rapidly in an intermediate regime flow and to develop the required morphology to establish efficient movements earlier.

KEY WORDS: swimming, ontogeny, body-caudal locomotion, Strouhal number, larvae

INTRODUCTION

In most fish, swimming corresponds to the propagation of a wave of increasing amplitude from head to tail (GRAY, 1933), which is commonly named the body/caudal fin locomotion (BCF) (BREDER, 1926; LINDSEY, 1978; VIDELER, 1993). Depending primarily on the parameter of size, undulatory movements generate thrust in a range of flow regimes, by exploiting viscous or inertial forces or both (VIDELER, 1993). The ratio between the viscous and inertial forces can be assessed by the Reynolds number (Re). At hatching, larvae are only a few millimeters long and the corresponding flow regime is dominated by viscous forces (Re values below 100) (MCHENRY & LAUDER, 2005; VIDELER, 2011). This means that larvae must use large body wave amplitudes along their whole body to enable them to exploit the viscous force optimally (WEBB & WEIHS, 1986). This set of movements corresponds to the anguilliform swimming mode (MÜLLER & VAN LEEUWEN, 2004; MAUGUIT et al., 2010a,b). Experiments showed that an increase in the viscosity of the medium induced an increase in the amplitude of the movement in the anterior part of the body (HORNER & JAYNE, 2008; DANOS, 2012). During growth, fish experience a gradual change from a viscous to an intermediate regime (Re > 300) and then from the intermediate to an inertial flow regime (Re > 1000) (MÜLLER & VIDELER, 1996; OSSE & VAN DEN BOOGAART, 2000; MCHENRY & LAUDER, 2005). Simultaneously, skeletal, muscular and nervous systems develop while new structures (i.e. fins) are recruited, and other structures

(i.e. yolk-sacs) are lost. These changes are important in setting physical limits to locomotor performance (WEBB, 1984), and are expected to affect the ontogeny of swimming (FUIMAN & WEBB, 1988). However, the developmental process driving the swimming capacity has received little attention. The kinematics of swimming in fish larvae has been studied in zebrafish *Danio rerio* (Hamilton, 1822) (FUIMAN & WEBB, 1988; MÜLLER & VAN LEEUWEN, 2004; FONTAINE et al., 2008; MÜLLER et al., 2008), the common carp *Cyprinus carpio* (L., 1758) (OSSE, 1990; OSSE & VAN DEN BOOGAART, 2000), the European plaice *Pleuronectes platessa* (L., 1758) (BATTY, 1981) and the Atlantic herring *Clupea harengus* (L., 1758) (BATTY, 1984). However, these studies only focused on a few larval stages (from 2 to 7) and did not provide a global view of the developmental cycle.

More recently, MAUGUIT et al. (2010a,b) more thoroughly examined the development of swimming by studying 21 and 23 larval stages in *Clarias gariepinus* (Burchell, 1822) and *Corydoras aeneus* (Gill, 1858), respectively. Both studies used a new kind of analysis that allows a better understanding of the changes in swimming during fish growth. This method is based on the work of VIDELER (1993). In theory, during one undulatory movement, each body part follows a pure sine-like trajectory when two conditions are observed: (1) the swimming speed is constant during the execution of one swimming movement and (2) the lateral amplitude of each body part is small (VIDELER, 1993). In practice, neither condition is met. First, the thrust oscillates during one tail-beat as the tail beats back and forth. Consequently, the swimming speed also fluctuates (MÜLLER & VAN LEEUWEN, 2004). Second, the body wave amplitude increases from the pivot point to the tail (VIDELER, 1981). The pivot point, located just behind the head, characterizes the position on the body where the smallest amplitude of lateral movement is usually observed. Consequently, the propulsive wave deviates moderately from a pure sine-like trajectory at this pivot point and more markedly at the tail, where the amplitude is maximal. Variations in swimming speed during one tail-beat are stronger in the viscous flow regime of small, slow swimmers than in the inertial flow regime of large, fast swimmers (MÜLLER & VAN LEEUWEN, 2004). In a viscous flow regime, large amplitudes of each body part are required to better exploit forces of the medium while in an inertial flow regime, smaller amplitudes allow better penetration in the water (BATTY, 1981).

Thus, we predict larvae may be unable to perform sine-shaped movements at hatching. During ontogeny, as body length and absolute swimming speed increase and morphological developments occur, we expect larvae to progressively improve their swimming ability towards sinusoidal movements.

Our aim is to use the method of MAUGUIT et al. (2010a) to describe the ontogeny of the swimming in *Dicentrachus labrax* (seabass) (L. 1758) from hatching to 104 days post-hatching. The data will then facilitate more comprehensive comparisons with the two species studied by MAUGUIT et al. (2010a,b): *Clarias gariepinus* and *Corydoras aeneus*. The two catfish species live in subtropical regions in freshwater. Both stay generally in quiet waters near the bottom (TEUGELS, 1986; BURGESS, 1992). At adult stage, the two species differ in their swimming mode, one using the anguilliform mode (*C. gariepinus*) and the other the carangiform mode (*C. aeneus*) (MAUGUIT et al., 2010a,b). *Dicentrachus labrax* generally favours turbulent environments in cold and temperate seawaters. Larvae hatch in the open sea and, once juveniles, drift towards the coast and estuaries (PICKETT & PAWSON, 1994). At adult stage, seabass use a subcarangiform swimming mode (PALOMARES, 1991; HERSKIN & STEFFENSEN, 1998). The differences between habitats and way of life should affect the growth and the rate of morphological development of the species and in this way the establishment of swimming behaviour. Being a marine fish living in cold/temperate water, the seabass should have slower growth and rate of morphological development than the two catfish species. We expect that the establishment of swimming in *D.*

labrax will take more time than in *C. gariepinus* and in *C. aeneus*.

MATERIALS AND METHODS

In this study the larval period was determined as the period between hatching and the ossification of the caudal fin. Once the caudal fin was ossified, fish were considered as juveniles. Larvae of *D. labrax* were bred at Aquanord hatchery (Gravelines, France) in a community tank filled with running seawater at a temperature of 15°C. Larvae were kept in the darkness until 216 hours post-hatching (hPH). Then, light was turned on with a photoperiod of 12h and larvae were fed with brine shrimps three times a day (*Artemia salina* L., 1758). Juveniles (whose caudal fin is ossified) were also bred in a community tank at a temperature of 20°C. Fish were sampled at different stages: 0, 4, 8, 12, 16, 20, 24, 32, 40, 48, 60, 72, 96, 120, 144, 168, 192, 216, 240, 264 and 288 hPH for larvae and 960, 1896 and 2496 hPH (respectively 40, 79 and 104 days post-hatching) for juveniles. For each stage, 15 individuals were sampled and were separated into three batches of five fish. In each batch, swimming was recorded at 500 frames s^{-1} with a high-speed digital video camera (RedLake MotionPro 2000; RedLake, San Diego, California, USA) from a dorsal view. Swimming sequence was recorded only once per batch to avoid studying the same individual twice. A total of three independent replicates was collected for each stage. Note that a sequence suitable for further analysis was defined when fish performed one complete undulatory movement in a straight direction and at a constant speed. For each swimming movement, the first three tail strokes were not recorded to avoid inclusion of acceleration movements.

Three tanks of variable dimensions were used: 7.5 cm × 2.5 cm, 14.5 × 8 cm, 123 × 8.5 cm respectively for larvae (3 to 5.6 mm TL), small juveniles (<20 mm TL) and large juveniles (>20 mm TL). The water level was always five times the fish height. Fish were free to move in all directions and at variable swimming speeds. The camera was mounted on a Stereozoom Microscope (Leica M10; Leica, Wetzlar, Germany) for larvae and equipped with a lens (Linos Mevis 25 mm, 1.6: 16; Linos; Munich, Germany) for juveniles. The two smallest tanks were lit from the top and the bottom (light reflected by a mirror) with two 240W Volpi 6000-1 cold light sources (Volpi, Schlieren, Switzerland) and optical fibers. The largest tank was lit from the top with two 1000W spotlights (IFF Q1250).

The analyses of sequences of the swimming movements were carried out with Midas software (RedLake, version 2.1.1). For larvae and juveniles, a total of 63 and nine sequences respectively were analyzed in an earth-bound frame of reference. The fish midline was divided into seven equal segments by selecting eight landmarks between the snout and the tail tip, *i.e.* at 0, 0.14, 0.29, 0.43, 0.57, 0.71, 0.86 and 1 TL (respectively LM1 to LM8, Fig. 1). A

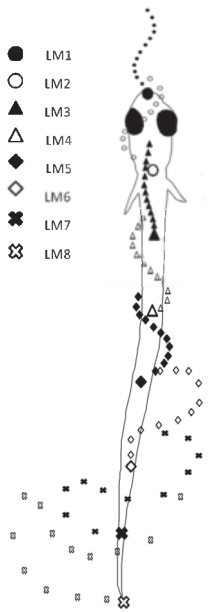

Fig. 1. – Drawing of a swimming movement executed by a seabass larva (*Dicentrarchus labrax*). The eight paths made up of different markers represent the trajectory of each landmark (LM1-LM8) during the execution of a complete undulatory swimming movement. The larger symbol of each type indicates the placement of the landmarks on the fish body.

preliminary study determined the useful number of landmarks. The use of eight landmarks allowed placing the second one near the pivot point (where the amplitude of the movement is the weakest along the body). The x-axis was defined as the direction of fish displacement and the y-axis was perpendicular to the x-axis. A transformation was done to move the first point of the trajectory of each landmark to the x-axis origin (x = 0). The aim of this transformation was to use the same referential for analyzing the motions of each landmark independently of its position on the fish.

For each sequence, direct and indirect parameters were selected to describe the swimming movement. The direct parameters were total fish length (TL; mm), relative swimming speed (U; TLs^{-1}), tail-beat frequency (f; s^{-1}), the wavelength of the propulsive wave (λ) and the maximal amplitude movement of each landmark ($A_{1\text{-}8}$; %TL).

The indirect parameters were the three indices used by MAUGUIT et al. (2010b). The first index made it possible to assess the sinusoidal trajectories of the swimming movement. From a distribution of the observed values of x, and knowing the movement amplitude ($A_{1\text{-}8}$) and its wavelength, a theoretical sinusoid could be calculated for the various landmarks at each developmental stage. The sinusoidal function linking y_{th} (theoretical y) and x is $y_{th} = A \sin(\omega x+\varphi)$, where A is the amplitude (in mm), ω the pulsation (in radian mm^{-1}), and φ the initial phase (in radians). The amplitude (A) and the pulsation (ω) were determined from the observed coordinates: $A = y_{max}$ and $\omega = 2\pi T_x^{-1}$, where y_{max} is the maximum amplitude observed during one tail-beat and T_x is the period of motion. For each landmark, the y_{th} values were calculated by varying φ between 0 and 2π by increments of 0.01 radian (this yields 628 theoretical sinusoids) to obtain the best fit between the observed and theoretical curves. The φ value of the theoretical sinusoid having the best fit (the highest r^2) with the observed motion was then selected. These sinusoids correspond to the theoretical ideal trajectories that each landmark should follow during execution of a complete undulatory movement (i.e. to the situation that should be observed at the adult stage). The paths observed for the various landmarks throughout ontogeny were compared with these theoretical sinusoids by determining the coefficient of determination (r^2) between the two curves. The coefficients of determination of LM1-LM8 ($r^2_{1\text{-}8}$) provided an objective index of the similarity between this motion and the adult sinusoid motion for each landmark placed on a fish. The r^2_{mean}, the mean of the r^2_1 to r^2_6, provided a global index of the body movement profile at a specific developmental stage. Swimming movements were considered to be sinusoidal when r^2_{mean} was ≥ 0.95. Landmarks 7 and 8 were not taken into account for the r^2_{mean}. Landmarks 7 and 8 were on the caudal region. This region is not yet developed in larvae (no ray-finned caudal fin and no intrinsic muscles), which therefore are unable to fully control their tail-tip movements. However the caudal fin follows a better sinusoidal path once developed (in juveniles); the caudal fin has intrinsic muscles that are able to alter the movement (LAUDER, 1989, 2000). In consequence, the caudal region does not behave the same way as the rest of the body. For this reason the corresponding r^2 were not taken into account for the r^2_{mean}.

The coefficient of variation of r^2 (CV), the second index, was calculated with the r^2_1-r^2_6 values to gauge whether, at a given developmental stage, the movement appeared to have the same level of organization in different parts of the body.

The third index used was the Strouhal number:

$$[\text{Formula 1}]\ St = \frac{f \times A_8}{U^{-1}}$$

where f is the tail-beat frequency, A_8 the maximum amplitude of the caudal fin and U the swimming speed. The St value describes how fast the tail is flapping relative to how fast the fish is swimming. The value of this index is dependent on the Re values (BORAZJANI & SOTIROPOULOS, 2008, 2009). For adult fish whose corresponding

Re values are very high, the swimming efficiency is optimal when the *St* values range from 0.25 to 0.45 (BORAZJANI & SOTIROPOULOS, 2008, 2009; LAUDER & TYTELL, 2006; TAYLOR et al., 2003). But for fish whose corresponding Re values are only 300, the optimal *St* values go down to 1.3 (BORAZJANI & SOTIROPOULOS, 2008, 2009).

Other parameters about fish morphology and flow regime were also calculated: yolk-sac volume (Vv) and Reynolds number (Re). The shape of the yolk-sac was assumed to be a prolate spheroid (BAGARINAO, 1986), and the volume was calculated as follows:

$$[\text{Formula 2}]\ Vv = (\frac{\pi}{6}) \times L_v H^2$$

where L_v and H are respectively the length and the height of the yolk-sac. This parameter was measured on photos using Vistametrix version 1.34 (SkillCrest LLC, Tucson, Arizona, USA).

The effects of size, swimming speed and yolk-sac volume (independent variables) on r^2_{mean}, CV, *St* and the amplitudes of LM1 to LM8, were investigated by multiple polynomial regressions of the third degree (the use of a higher degree did not improve the accuracy of the analysis). The best-fit model was identified in a stepwise forward-selection manner and was selected based on the lowest *p*-value. Only significant values were included in the models (Student's *t* test, $p < 0.05$) and presented in the results. In graphs showing effects of size and swimming speed on r^2_{mean}, CV and *St* values, data are presented in a surface plot where the size is on the x axis, the swimming speed is on the y axis, and the values of the dependent variable are provided by a color code. The surface that fitted best to the points of observation was determined by the weighted least squares method (MCLAIN, 1974). Nonparametric correlation (Spearman) was also determined between Reynolds and Strouhal numbers.

RESULTS

Three movements from three different fish were analyzed for each stage. The sample is similar to the ones of the two studies of MAUGUIT et al. (2010a,b) (72 sequences for *D. labrax*, 93 for *C. gariepinus* and 73 for *C.aeneus*).

Swimming ontogeny in the larval period (from hatching to 288 hPH)

Larvae measured 3.3±0.2 mm (n = 3) at hatching and were observed until they grew to 5.5±0.1mm (= 288 hPH; n = 3). The yolk-sac (initially 0.4±0.01 mm^3, n = 3) was totally resorbed between 96 and 120 hPH. Pectoral fins appeared at a size of 4.93±0.21 mm (96 hPH; n = 3). Independent of age, size and morphology, the swimming bouts could be split into two groups swimming at different speeds. According to the terminology used in BLAXTER (1969), the first group used a steady swimming speed (1.31 to 4.88 TLs^{-1}) (n = 50) while the second performed a burst of swimming (12.73 to 27.62 TLs^{-1}) (n = 13). None of the larvae swam at the intermediate speed, between 4.9 and 12.73 TLs^{-1}. Tail-beat frequencies were 20.47±3.69 Hz for the steady swimming group and 49.07±5.39 Hz for the burst of swimming group. In burst of swimming larvae, the six fastest bouts (24 to 27.62 TLs^{-1}) were in an intermediate regime (Re > 300). All the other recorded swimming bouts were in a viscous flow regime (Re ≤ 300).

Swimming movements were observed at hatching. These movements were not completely sinusoidal (r^2_{mean}=0.77±0.17), but r^2_{mean} values continuously increased with growth (Fig. 2A; $F_{[4,58]} = 24.170$, $p < 0.001$). At the size of 5.2 mm, all larvae were able to perform sinusoidal movements ($r^2_{mean} \geq 0.95$) while swimming speed ranged from 1.9 to 23.23 TLs^{-1} (Fig. 2A). Moreover, independent of size, there was a strong correlation between a sinusoidal movement and swimming speed (Figure 2A; $F_{[4,58]} = 24.170$, $p < 0.001$): all larvae with a burst of swimming (>12 TLs^{-1}) performed sinusoidal movements independent of size (Fig. 2A). During ontogeny, the sinusoidal swimming motion was established first in the middle part of the body near the pivot point (LM3-LM4). The same acquisition was

then observed along almost all the rest of the body (LM1-LM2; LM5). After larvae reached a size of 5.2 mm, all body landmarks (LM1 to LM6) exhibited sinusoidal paths (Fig. 3A). This variation in the time of acquisition of sinusoidal movement for different parts of the body induced high values of CV in larvae (ca 12%) (Fig. 2B). Independent of size, fish swimming at least at 12 TLs^{-1} (= burst of swimming) show CV around 2% (Fig. 2B; $F_{[3,59]} = 7.6278$, $p<0.001$), with all the body parts (LM1-LM6) exhibiting sinusoidal trajectories. Although the r^2_7 and the r^2_8 values increased regularly with growth and with speed ($F_{4,58} = 13.209$, $p < 0.001$ for r^2_7 and $F_{4,58} =$

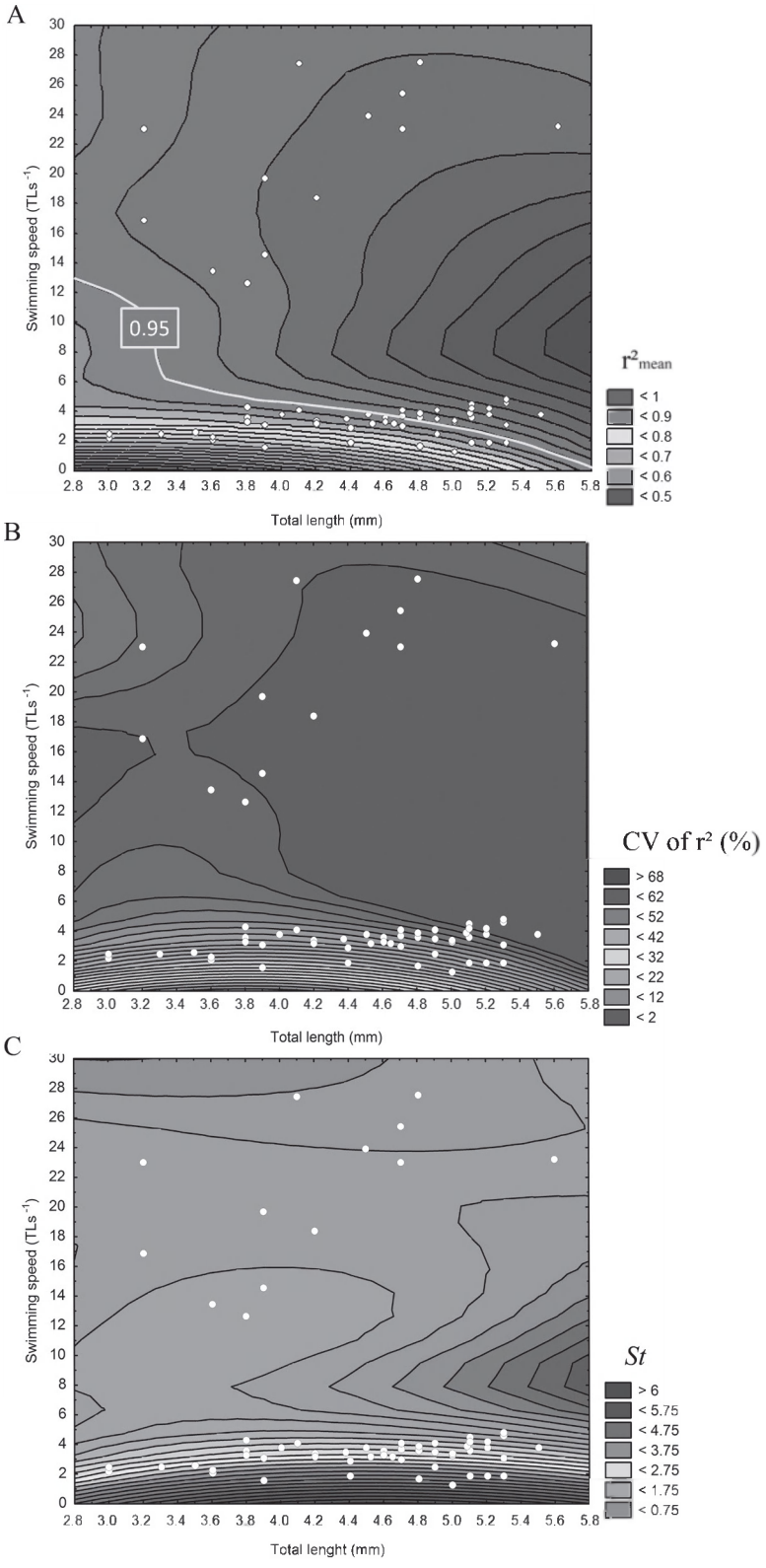

Fig. 2. – Contour plot representing the changes in (A) mean coefficient of determination (r^2_{mean}), (B) coefficient of variation of r^2 (CV of r^2) and (C) Strouhal number (*St*) as a function of the total fish length (TL) and relative swimming speed (U) of larvae of seabass (*Dicentrarchus labrax*). The index values are given by the colour code. The white circles represent observations made during the present study. Each circle corresponds to one fish. These data were used to fit the isoclines by means of the weighted least square distance method. In A the line represents the threshold value of 0.95. White circles located to the left of this line correspond to fish that did not execute fully sinusoidal swimming movements, whereas those to the right of this line correspond to fish with sinusoidal swimming movements.

11.060, $p < 0.001$ for r^2_8), sinusoidal movements were rarely observed at the level of the tail.

At hatching, larvae swam with high Strouhal numbers (> 2), and this index did not change significantly at the end of the larval period studied (Fig. 2C; $F_{[3,59]} = 27.527$, $p < 0.001$). During the period studied, larvae did not grow very much and so Re values did not differ substantially:

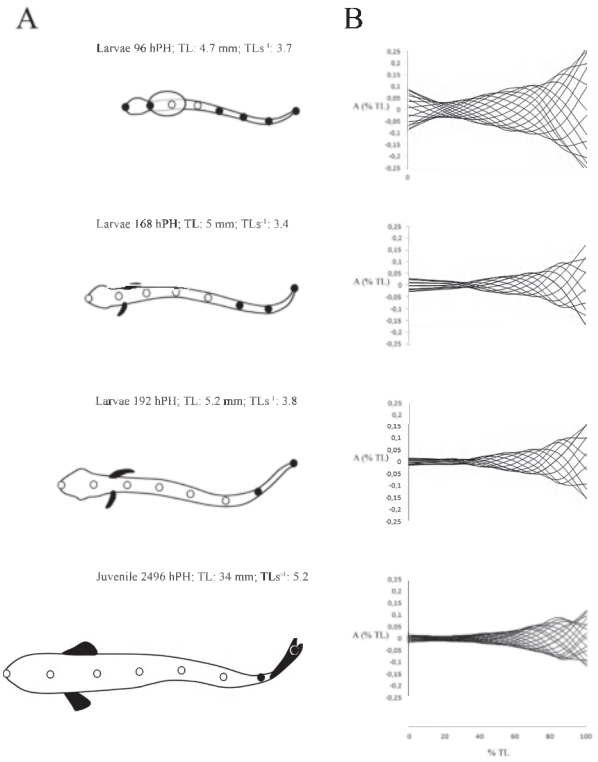

Fig. 3. – **A**. Representation of four stages: three larval and one juvenile. The eight landmarks used in the analysis of the swimming movement are indicated on the midline of each fish. White landmarks indicate that all fish from the size indicated reached at least a value of 0.95 for the corresponding r^2. **B**. Midline kinematics of seabass (*Dicentrarchus labrax*) larvae and juveniles during cyclic swimming at different stages of ontogeny. The superimposed midlines (time step 4 ms) of one tail-beat cycle show the amplitude envelope of the body wave. Each amplitude envelope corresponds to the fish represented by the black shape. The amplitude is expressed as a proportion of total fish length (TL), the *x* axis representing the total fish length in percentage.

from 20±3.5 (n = 3) at hatching to 94±17 (n = 3) at 288 hPH (only for steady swimming). It is well known that *St* values are strongly correlated with Re values (BORAZJANI & SOTIROPOULOS, 2008), so no relation between size of larvae and *St* values was discovered. However, a strong correspondence was observed with swimming speed: the values of Re increased considerably for larvae with bursts of swimming (Re = 323±160; n = 13), inducing a decrease in *St* number values (1.12±0.28) (Fig. 2C; $F_{[3,59]} = 27.527$, $p < 0.001$).

During growth, the relative amplitudes of the different body parts (LM1-6) decreased in parallel to a better sine-shaped swimming mode (Fig. 3B; $F_{[2,60]} =$ 51.144 (LM1); 38.647 (LM2); 54.265 (LM3); 51.700 (LM4); 33.702 (LM5); 40.640 (LM6); $p<0.001$). VIDELER (1993) and BREDER (1926) defined a subcarangiform mode as a swimming movement where the amplitude increases significantly in the posterior part of the body and where between 0.5 and 1 wavelength of propulsive wave (λ) is observed in the fish body. Despite the decrease in the amplitude movement of the LM1-6 during growth, all larvae swam with more than one λ on the body. So, the transition from an anguilliform to a subcarangiform mode was not yet complete. Except at the caudal tip (LM8), the amplitude of movement increased with swimming speed ($F_{[2,60]} =$ 51.144 (LM1); 38.647 (LM2); 54.265 (LM3); 51.700 (LM4); 33.702 (LM5); 40.640 (LM6); 29.592 (LM7); $p < 0.001$).

The impact of yolk-sac resorption was also studied on the three indices and lateral displacements of the body during swimming movements (A_1 to A_8), but no significant relationship was found.

Swimming mode in juvenile stages (960-2496 hPH)

The size of the juveniles ranged from 14.3 to 34.2 mm, and all had a fully ossified caudal fin. Their swimming speed ranged from 2.32 to 23.4 TLs^{-1} with a tail-beat frequency of 14.8±10.72 Hz. Juveniles between 14 and 19 mm swam in the intermediate flow regime with Re values

from 509 to 848. Larger juveniles (25 to 34 mm) evolved in the inertial flow regime with Re values from 5242 to 13301.

The r^2_{mean} was always higher than 0.95 (0.98±0.01), and the CV was low (1.84±0.94 %). Although the caudal fin followed better sinusoidal paths than in larvae, the threshold value of 0.95 was not always reached. The Strouhal numbers ranged from 0.48 to 1.58, with the lowest values being found for juveniles swimming in an inertial regime. Juveniles performed swimming movements with an important increase of the amplitude in the posterior part of the body and with a propulsive wave between 0.5 and 1 wavelength. Therefore, the transition to a subcarangiform mode occurred between the larval and juvenile stages.

DISCUSSION

All *Dicentrarchus labrax* larvae start their life swimming with an anguilliform motion that is functional in all types of hydrodynamic flow regimes (GRAY & HANCOCK, 1955, LIGHTHILL, 1969, WEBB & WEIHS, 1986). In addition, the anguilliform mode is used by all fish larvae, no matter what mode they eventually use as adults (OSSE & VAN DEN BOOGAART, 2000; MÜLLER & VAN LEEUWEN, 2004; MAUGUIT et al., 2010a,b). During growth, swimming movements become more sinusoidal, made up of movements having less relative amplitude. The *St* values do not change with size in larvae but are substantially reduced in juveniles that pass into the intermediate regime flow and have a subcarangiform swimming mode. However, it appears that swimming speed has a strong influence on all parameters studied, regardless of size and morphological development.

Previous studies on the ontogeny of swimming abilities in different fish species concerned only a few larval stages (BATTY, 1981, 1984; FUIMAN & WEBB, 1988, OSSE, 1990, OSSE & VAN DEN BOOGAART, 2000; FONTAINE et al., 2008; MÜLLER et al., 2008), restricting the accurate comparisons between taxa. The study on zebrafish by MÜLLER et al. (2004) dealt with several larvae stages but none of the different indices used in our studies were used, so comparisons are difficult to make. For this reason, we can only compare our data to the data for *Clarias gariepinus* and *Corydoras aeneus* (MAUGUIT et al., 2010a,b) for which many developmental stages were also studied.

However, the biology of these three species differs in several points that can influence the establishment of swimming behaviour. *Dicentrarchus labrax* is a marine fish that lives in cold/temperate water. As a consequence, larval seabass were reared in seawater at 15°C. Being subtropical catfish species, larvae of *C. gariepinus* and *C. aeneus* were reared in freshwater at 28 and 25°C, respectively (MAUGUIT et al., 2010a,b). The time of hatching after fertilization differs between species; 24h only for *C. gariepinus*, 72h for *C. aeneus* (MAUGUIT et al., 2010a,b) and 96h for *D. labrax*. The temperature and the salinity are both ecological factors that act directly through receptors to increase or decrease growth (BOEUF et al., 2001), while the time between fertilization and hatching can have an effect on the morphological stage of larvae at hatching. The differences between these parameters can, probably, largely explain the differences observed in ontogeny of swimming development in the three species studied.

Figure 4 provides a panel contrasting the main modifications in swimming abilities between the three species that live in two different environments and have different modes of swimming in the adult stage.

At hatching, only *C. aeneus* has pectoral fins and is the only species to perform sinusoidal swimming (MAUGUIT et al, 2010b). *Clarias gariepinus* larvae hatch the earliest after fertilization and are unable to perform any swimming at this stage (MAUGUIT et al., 2010a). *Dicentrarchus labrax* larvae spend the longest time in the egg phase, but live in colder water with higher salinity, which should decrease their developmental, growth rate. At hatching, *D.*

labrax cannot perform sinusoidal swimming (r^2 = 0.77±0.17) (Fig. 4). In various species it has been observed that oscillations in the anterior part of the body during swimming movements in larvae decrease once the pectorals fins appear (BATTY, 1981, OSSE, 1990, THORSEN et al., 2004). The present study confirms this statement. In *D. labrax*, pectoral fins appear at 4.93±0.21 mm and almost all the body (LM1-LM5) follows a sinusoidal path from a size of 5 mm (Fig. 3A).

A common characteristic in the ontogeny of swimming in the three species is a progressive decrease in the amplitude of movement in the anterior part of the body. The amplitudes of LM1 to LM4 for catfishes and of LM1 to LM5 for the seabass decrease by 50% in the first days after hatching (Fig. 4). This amplitude reduction was earlier thought to explain the change in the *St* number (MAUGUIT et al. 2010a,b). However, this assumption is not verified in *D. labrax* (Fig. 4). The *St* number has mostly been studied in fish moving in an inertial regime (TAYLOR et al., 2003, TYTELL, 2004; LAUDER & TYTELL, 2006). More recently, studies by BORAZJANI & SOTIROPOULOS (2008, 2009) showed the *St* number is inversely related to Re values: an Re of 300 (intermediate regime) corresponds to an optimal *St* number of 1.3, and an Re of 4000 (inertial regime) corresponds to an optimal *St* of 0.6. This correlation between Re and *St* is also observed in our results (Fig. 5). The fact that changes in *St* number are first of all related to changes in Re number could explain why catfish species reach a low *St* number faster than seabass (Fig. 4). Because catfish species

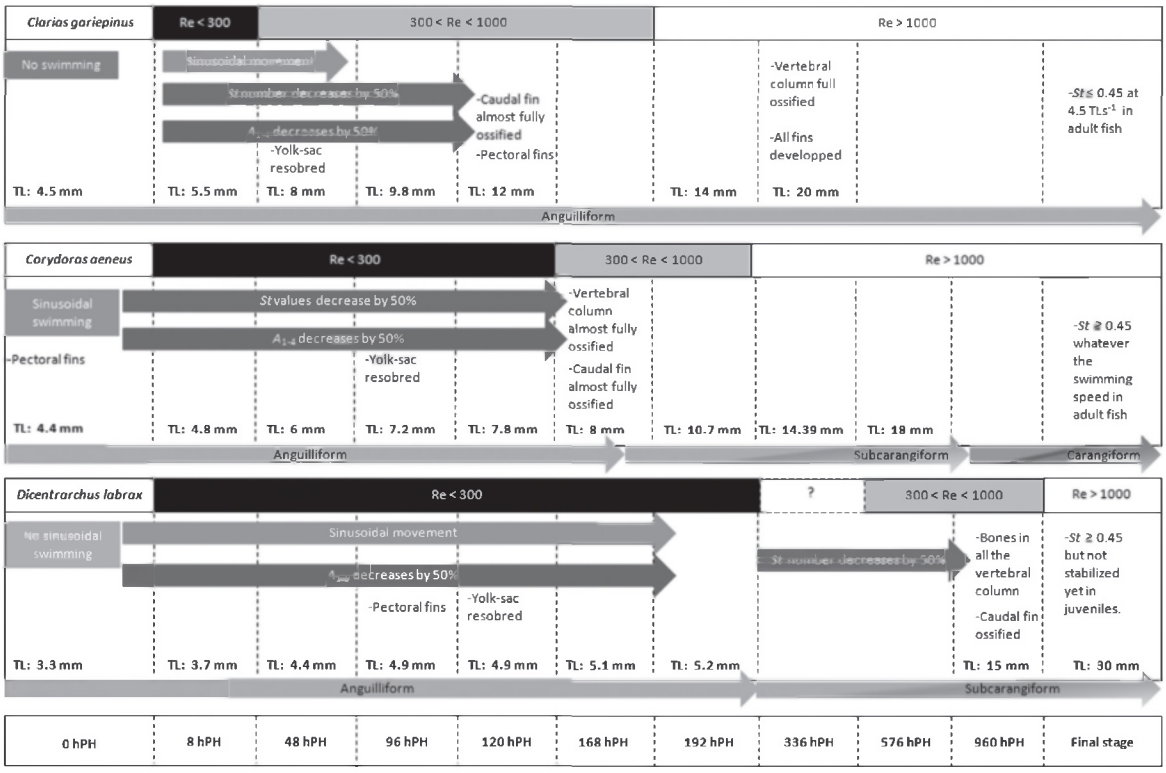

Fig. 4. – Major steps in the swimming ontogeny in *Clarias gariepinus*, in *Corydoras aeneus* and in *Dicentrarchus labrax*. The data on the catfishes are obtained from the studies of MAUGUIT et al; (2010a,b). The acquisition of sinusoidal swimming, the evolution of *St* values and the changes in swimming mode are expressed in relation to age, size, regime flow and morphological changes in the three species. For *D. labrax*, the transition between the viscous and the intermediate regime is lacking. For each species, all morphological changes cited were observed in the fish in the corresponding studies on ontogeny of swimming and not from the literature. The gradual transition between different swimming modes is indicated by bicolour arrows.

grow faster, they are able to earlier reach high Re values and the intermediate regime at a cruise speed. Having slower growth, seabass larvae are restricted longer to a small size and to a viscous flow. In this flow, *D. labrax* larvae need to swim at high frequency (22.85±2.09 Hz; n = 63), which decreases their efficiency. Consequently, the major decrease in *St* does not occur until the first juvenile stage studied (ca 15 mm TL: 960 hPH), corresponding to swimming in an intermediate regime at a cruising speed (Fig. 4). In this regime flow, the total drag decreases, the tail-beat frequency is slower (14.8±10.72 Hz; n = 9) and the swimming efficiency improves (*St* = 0.095±0.04; n = 9). Additionally to the change in regime flow, the ossification of caudal fin rays corresponds to an important decrease in tail-beat frequency and in *St* number in all the species (Fig.4). The ossification of the vertebral column and caudal fin increases the stiffness of the body and allows better force transmission (BATTY, 1981; LONG et al., 1994; MCHENRY et al., 1995; HALE, 1999). For *C. aeneus* and *D. labrax*, this ossification also occurs before the transition in swimming mode, demonstrating that a rigid axis is required for a subcarangiform and carangiform mode.

The swimming speed appears to strongly affect the values of r^2_{mean}, CV and *St* in *D. labrax*. All larvae swimming at high speed are able to perform a sinusoidal swimming motion ($r^2_{mean} \geq 0.95$) with a constant motion along the length of the body (CV = 2.45±1.99; n = 13). According to the study by BUDICK & O'MALLEY (2000) on the fast swimming speed in *Danio rerio*, the ability in larvae to execute very fast movements could be due to a good synchronization of motoneurons firing along the body. This improved synchronization could partially explain the good coordination along the body during fast swimming movements. Larvae also show decreasing *St* number with increasing swimming speed, which is related to the way the Re number varies. At high speed, Re number increases considerably for swimming larvae. Consequently, total drag decreases and efficiency increases (*St* number decreases).

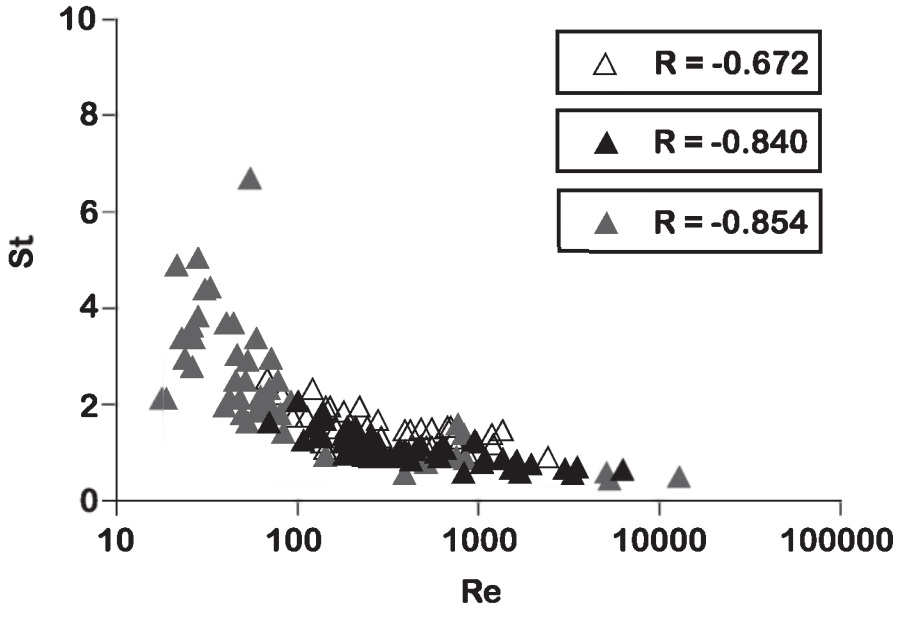

Fig. 5. – Correlation between *St* and Re values in *Clarias gariepinus* (in white), *Corydoras aeneus* (in dark grey) and *Dicentrarchus labrax* (in light grey). The *x* axis is presented in $\log_{10}$. The values of the correlation (R) are indicated.

CONCLUSION

The gradual establishment of adult swimming movement is not the same between the three species studied, but varies according to morphological development and growth rate. However it does follow the same pattern: 1) they transition from a viscous to an intermediate and then to an inertial flow regime; 2) they begin with an anguilliform swimming mode; 3) for the three species the decrease in tail-beat frequency and in *St* correspond to an increase in Re and are correlated to ossification of caudal fin rays.

Being a marine fish, *D. labrax* growth rate is lower than that of the two catfishes. Therefore sea bass larvae stay in low Re values longer and have consequently high *St* values during their larval period. However the viscous flow regime does not impede the establishment of a sinusoidal movement since stabilization of r^2_{mean} and CV occur in this regime.

ACKNOWLEDGEMENTS

Funding for this research was provided by «Fonds pour la Formation à la Recherche dans l'Industrie et dans l'Agriculture». All experiments were approved by the local ethics committee. We are grateful to Stan Laureau from *Aquanord* (Gravelines, France) who enabled us to work in his hatchery. We thank the branch editor D. Adriaens and the two anonymous reviewers for their comments. This is the AFFISH publication n°7.

REFERENCES

BAGARINAO T (1986). Yolk resorption, onset of feeding and survival potential of larvae of three tropical marine fish species reared in the hatchery. Marine Biology, 91: 449-459. http://dx.doi.org/1007/BF00392595

BATTY RS (1981). Locomotion of plaice larvae. Symposia of the Zoological Society of London, 48: 53-69.

BATTY RS (1984). Development of swimming movements and musculature of larval herring (*Clupea harengus*). Journal of Experimental Biology, 110: 217-229.

BURGESS W (1992). Colored atlas of miniature catfish. Every species of *Corydoras*, *Brochis* and *Aspidoras*. T.F.H. Publications, Inc., Neptune City, New Jersey (USA).

BLAXTER JHS (1969). Development eggs and larvae. *In*: W. HOAR & D. RANDALL (eds), Fish Physiology, Elsevier, 3: 177-252.

BOEUF G & PAYAN, P (2001). How should salinity influence fish growth? Comparative Biochemistry and Physiology Part C, 130: 41-423.

BORAZJANI I & SOTIROPOULOS F (2008). Numerical investigation of the hydrodynamics of carangiform swimming in the transitional and inertial flow regimes. Journal of Experimental Biology, 211(10): 1541-1558. http://dx.doi.org/10.1242/jeb.015644

BORAZJANI I & SOTIROPOULOS F (2009). Numerical investigation of the hydrodynamics of anguilliform swimming in the transitional and inertial flow regimes. Journal of Experimental Biology, 212(4): 576-592. http://dx.doi.org/10.1242/jeb.025007.

BREDER CM (1926). The locomotion of fishes. Zoologica, 4: 159-256.

BUDICK S A & O'MALLEY DM (2000). Locomotor repertoire of the larval zebrafish: swimming, turning and prey capture. Journal of Experimental Biology, 203: 2565-2579.

DANOS N (2012). Locomotor development of zebrafish (*Danio rerio*) under novel hydrodynamic conditions. Journal of Experimental Zoology, 317:117–126.

FONTAINE E, LENTINK D, KRANENBARG S, MÜLLER UK, VAN LEEUWEN JL, BARR A H & BURDICK JW (2008). Automated visual tracking for studying the ontogeny of zebrafish swimming. Journal of Experimental Biology, 211(8): 1305-1316. http://dx.doi.org/10.1242/jeb.010272

FUIMAN L A & WEBB PW (1988). Ontogeny of routine swiming activity and performance in *zebra danios* (Teleostei, Cyprinidae). Animal Behaviour, 36(1): 250-261. http://dx.doi.org/10.1016/S00033472(88)80268-9

GRAY J (1933). Studies in animal locomotion: I. The movement of fish with special reference to the eel. Journal of Experimental Biology, 10: 88-104.

GRAY J & HANCOCK GJ (1955). The propulsion of sea-urchin spermatozoa. Journal of Experimental Biology 32: 775-801.

HALE M E (1999). Locomotor mechanics during early life history: Effects of size and ontogeny on fast-start performance of salmonid fishes. Journal of Experimental Biology, 202(11): 1465-1479.

HERSKIN J & STEFFENSEN JF (1998). Energy savings in sea bass swimming in a school: measurements of tail beat frequency and oxygen consumption at different swimming speeds. Journal of Fish Biology, 53: 366-376.

HORNER AM & JAYNE BC (2008). The effects of viscosity on the axial motor pattern and kinematics of the African lungfish (*Protoptetus annectens*) during lateral undulatory swimming. The journal of Experimental Biology, 211: 1612-1622. http://dx.doi.org/10.1242/jeb.013029

LAUDER GV (1989). Caudal Fin Locomotion in Ray-Finned Fishes: Historical and Functional Analyses . American Zoologist, 29: 85-102.

LAUDER GV (2000). Function of the Caudal Fin During Locomotion in Fishes: Kinematics, Flow Visualisation, and Evolutionary Patterns. American Zoologist, 40: 101-122.

LAUDER GV (2006). Hydrodynamics of undulatory propulsion. *In*: E. SHADWICK & GV LAUDER (eds), Fish Biomechanics, Elsevier, New York: 425-468.

LIGHTHILL MJ (1969). Hydromechanics of aquatic animal propulsion. Annual Review of Fluid Mechanics, 1(1): 413-446. http://dx.doi.org/10.1146/annurev.fl.01.0110169.002213

LINDSEY CC (1978). Form function and locomotory habits in fish. *In*: W. HOAR & D. RANDALL (eds), Fish Physiology, Academic Press, New York, 7: 1-100.

LONG JH, MC HENRY MJ & BOETTICHER NC (1994). Undulatory swimming: How traveling waves are produced and modulated in sunfish (*Lepomis gibbosus*). Journal of Experimental Biology, 192(1): 129-145.

MAUGUIT Q, GENOTTE V, BECCO C, BARAS E, VANDEWALLE N & VANDEWALLE P (2010a). Ontogeny of swimming movements in the Catfish *Clarias gariepinus*. The Open Fish Science Journal, 3: 16-29. http://dx.doi.org/10.2174/1874401X01003010016

MAUGUIT Q, OLIVIER D, VANDEWALLE N & VANDEWALLE P (2010b). Ontogeny of swimming movements in bronze corydoras (*Corydoras aeneus*). Canadian Journal of Zoology, 88: 378-389. http://dx.doi.org/10.1139/Z10-012

MCHENRY MJ & LAUDER GV (2005). The mechanical scaling of coasting in zebrafish (*Danio rerio*). Journal of Experimental Biology, 208 (12): 2289-2301. http://dx.doi.org/10.1242/jeb.01642

MCHENRY MJ, PELL CA & LONG JH (1995). Mechanical control of swimming speed-stiffness and axial wave-form in undalating fish models. Journal of Experimental Biology, 198(11): 2293-2305.

MCLAIN DH (1974). Drawing counturs from arbitrary data points. Computer Journal, 17: 318-324.

MÜLLER UK & VIDELER JJ (1996). Inertia as a 'safe harbour': Do fish larvae increase length growth to escape viscous drag? Reviews in Fish Biology and Fisheries, 6: 353-360.

MÜLLER UK & VAN LEEUWEN JL (2004). Swimming of larval zebrafish: ontogeny of body waves and implications for locomotory development. Journal of Experimental Biology, 207(5): 853-868. http://dx.doi.org/10.1242/jeb.00821

MÜLLER UK, VAN DEN BOOGAART JGM & VAN LEEUWEN JL (2008). Flow patterns of larval fish: undulatory swimming in the intermediate flow regime. Journal of Experimental Biology, 211(2): 196-205. http://dx.doi.org/110.1242/jeb.005629. 10.1242/jeb.005629

OSSE JWM (1990). Form changes in fish larvae in relation to changing demands of function. Netherlands Journal of Zoology, 40(1): 362-385. http://dx.doi.org/10.1163/156854289X00354

OSSE JWM & VAN DEN BOOGAART JGM (2000). Body size and swimming types in carp larvae; effects of being small. Netherlands Journal of Zoology, 50 (2): 233-244.

PALOMARES MLD (1991). La consommatíon de nourriture chez les poissons: étude comparative, mise au point d'un modèle prédictif et application à l'étude des réseaux trophiques. Ph D Thesis, Institut National Polytechnique, Toulouse.

PICKETT GD & PAWSON MG (1994). Seabass biology, exploitation and conservation. Chapman and Hall, Fish and Fisheries, 12.

TAYLOR GK, NUDDS RL & THOMAS ALR (2003). Flying and swimming animals cruise at a Strouhal number tuned for high power efficiency. Nature, 425(6959): 707-711. http://dx.doi.org/710.1038/nature02000.

TEUGELS, G. (1986). A systematic revision of the African species of the genus *Clarias* (Pisces: Clariidae). Annales Musee Royal de l`Afrique Centrale, 247: 199-247.

THORSEN DH, CASSIDY JJ & HALE ME (2004). Swimming of larval zebrafish: fin-axis coordination and implications for function and neural control. Journal of Experimental Biology, 207(24): 4175-4183. http://dx.doi.org/10.1242/jeb.01285

TYTELL ED (2004). The hydrodynamics of eel swimming II. Effect of swimming speed. Journal of Experimental Biology, 207(19): 3265-3279. http://dx.doi/org/10.1242/jeb.01139

VIDELER JJ (1981). Swimming movements, body structure and propulsion in cod *Gadus morhua*. Symposia of the Zoological Society of London, 48: 1-27.

VIDELER JJ (1993). Fish swimming. Chapman and Hall, London.

VIDELER (2011). An opinion paper: emphasis on white muscle development and growth to improve farmed fish flesh quality. Fish Physiology and Biochemistry, 37: 337-343. http://dx.doi.org/10.1007/s10695-011-9501-4

WEBB PW (1984). Form and function in fish swimming. Scientific American, 251: 72-82.

WEBB PW & WEIHS D (1986). Functional locomotor morphology of early life history stages of fishes. Transactions of the American Fisheries Society, 115(1): 115-127.

Received: November 21st, 2012

Accepted: June 21st, 2013

Branch editor: Adriaens Dominique